World Journal of Engineering Research and Technology
WJERT
www.wjert.org
SJIF Impact Factor: 5.218

CHARACTERIZATION OF UNKNOWN URANIUM CONTAINING MATERIAL FOR NUCLEAR SAFEGUARDS AND SECURITY PURPOSES

S. Shawky*

Egyptian Nuclear & Radiological Regulatory Authority, ENRRA.

Article Received on 06/09/2019 **Article Revised on 09/09/2019** **Article Accepted on 12/09/2019**

***Corresponding Author**
S. Shawky
Egyptian Nuclear & Radiological Regulatory Authority, ENRRA.

ABSTRACT

This paper investigates the applicability of material fingerprints (nuclear forensics) for material origin identification. Samples of unknown grinded rocks, ores and ore concentrates were analysed. For their characterization, the concentrations of major, minor elements, uranium and their secular equilibrium progenies were studied. Uranium content and its isotopic ratios, do not fully characterize the tested material, while these signatures and levels of concentration can probably help in determining processes of production, the stage and the possible origin material. Major elements such as Na, Al, Mn, K, Ca, Fe and Mg were determined using Scanning Electron Microscope- Energy Dispersive X-ray Analyses (ESM-EDX), while minor elements such as Sr, Zr, Mn, Cr, Ni, Cu, Zn, La, Ce, Y, Nb, U, Th, Pb, and As were analysed using Inductively Coupled Plasma Atomic Emission spectrometer (ICP-AES). For chosen isotopes compositions were determined using Inductively Coupled Plasma Mass Spectrometer (ICP-MS) and γ spectrometric analysis. Results show difference between samples in trace elements content, reflecting the different origin of samples. Rare Earth Elements (REE) signature and abundance patterns were tested as predictive signatures since direct-comparison samples were not available. This predictive approach, although more challenging than direct comparison, proven to be a sensitive tool to define source of origin among fully unknown samples. This demands the need for national database and proper searching engine for correlating the unknown material to a certain origin listed in the reference database. The database should list the fingerprints of different uranium ores and the ore concentrates at each production stage.

KEYWORDS: Uranium ores, ore concentrate, nuclear safeguards, nuclear forensics, elemental impurities.

INTRODUCTION

The Nuclear Security Summit, identified the risk of nuclear terrorism as the most immediate and extreme threat to global security. State Regulatory Authorities (SRAs) are responsible for state's compliance with their non- proliferation international agreements and the development of State nuclear security regime to prevent illegal Nuclear Material (NM) acquisition and development of nuclear explosion device by non-State actors.

Natural uranium is the starting point of nuclear fuel cycle for nuclear energy production and for production of weapon grade nuclear material. For nuclear security and safeguards purposes, SRAs shall have mechanism to control and track all types of nuclear material within their territory, under States jurisdiction or carried out under its control anywhere, including the very front-end of the nuclear fuel cycle, as described in INFCIR 153 corrected.[1] This express the need to identify and characterize potential sources of uranium production in their States to be able to correlate any possible illegal trafficking of NM to its origin.

The illicit tracking database (ITDB) of the international atomic energy agency (IAEA) register cases of illicit trafficking of nuclear material the majority of which is low-grade uranium. One approach to identify the origin of the confiscated material is to compare its physical and chemical characteristics to known samples in national database.

In addition to uranium content, uranium-containing materials have other characteristics that contribute to their unique signatures. They include chemical composition, minor elements, isotopic composition of uranium and its decay series and elements other than U, physical properties, such as colour, grain size distribution, etc. It is likely that some of these characteristics or their combination might constitute a unique signature for uranium materials and identify their origin and the chemical process used for their production.

There are various routes and processes applied in mining and milling, which might affect the content of minerals, heavy metals and trace elements across the process and in the product. Fig. (1), presents the main routes of the uranium mining processes and possible chemical forms in the course of production. Iterations of purification and concentration steps are

aiming at increasing the uranium content and reducing impurities to the commercially acceptable values for uranium ore concentrate (UOC). According to ASTM standards specification, the minimum uranium content of UOC is 65 mass percentage uranium and the contribution of impurities varies from fraction of a percent to 8%, uranium basis.[2] This is one of the aspects used when investigating unknown materials.

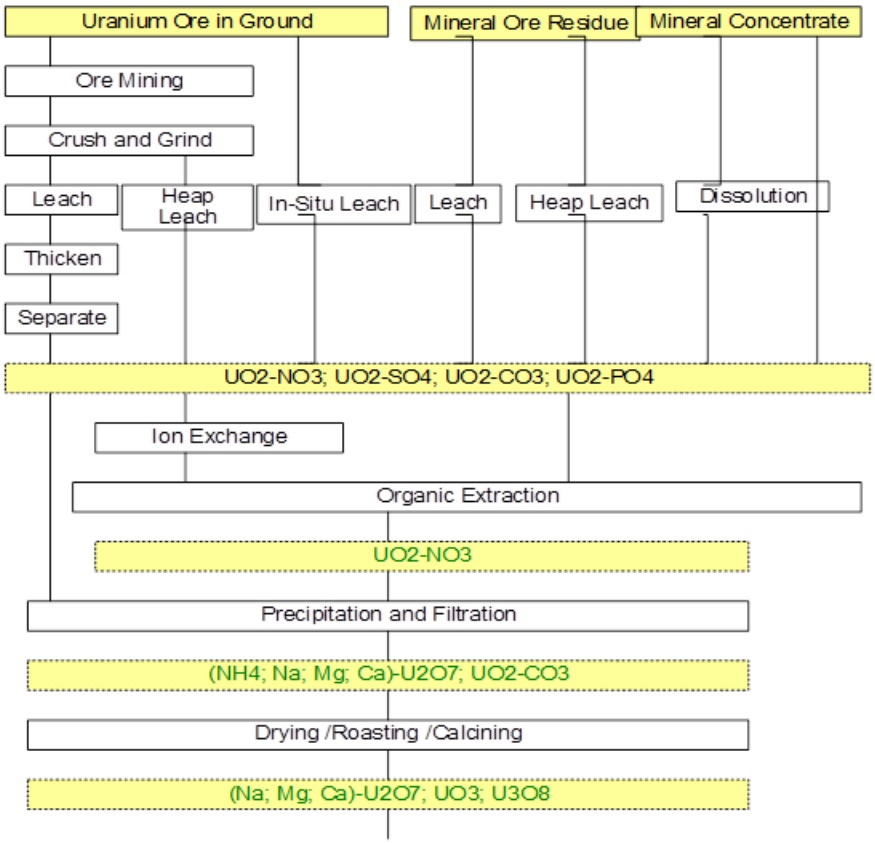

Fig. (1): Routes for mining uranium and relevant uranium compounds in the front-end processes.

Literatures reported that some of the observed signatures are related to origin, while others are related to products steering. Varga et al. presented typical example of the isotopic composition of uranium, strontium, neodymium and their rare earth elements (REE) composition.[3] In addition, Pb, Sr, S, Nd, O and U isotopic ratios are reported for the identification of source origin.[4-12] However, the isotopic composition of Pb could potentially vary between ore and ore concentrate. Pd becomes subject to separation from uranium during chemical processing of ores, or it could be introduced to samples during handling as well. Therefore, the isotopic ratios of other elements such as Nd and Sr are used to support the determination of origin samples.[9]

Uranium is primordial radionuclide with three naturally occurring isotopes; ^{238}U, ^{235}U and ^{234}U with half-life times of 4.5 10^9 y, 7.0 10^8 y and 2.5 10^5 y respectively. The ratio of $^{235}U/^{238}U$ was reported to be generally consistent while the ratio of $^{234}U/^{238}U$ is varying because of weathering and some geochemical effects such as alpha-recoil during ^{238}U decay, possible damage to the crystal structure, which may result in movement of ^{234}U out of minerals.[22-23] The ratio $^{230}Th/^{234}U$ chronometer is usually used for age determination of uranium materials. The age can be calculated as follows:

$$t = \frac{1}{\lambda p - \lambda d} \ln 1 - \frac{Nd}{Np} \cdot \frac{\lambda d - \lambda p}{\lambda p}$$

Where λ_d and λ_p the decay constants of daughter and parent nuclides,

N_d/N_p is the ratio of the daughter and parent nuclides in the sample, also called chronometer

t; is the passed time since the separation of the radionuclides.

As the REE, chemical properties are very similar; their relative abundances can relatively remain unchanged and not affected during concentration of uranium or by metamorphic processes. Therefore, they could provide information on the source of uranium bearing ores.[13] Kenton et al,[14] also proposed that REE abundance patterns may be used, as predictive signatures should direct-comparison samples be unavailable. The predictive approach is more challenging than the comparative method. Concentrates processed from certain ores convey their REE pattern.[3]

In this study, twelve samples of unknown rocks, ore and ore concentrates were analysed. For their characterization, the concentrations of major, minor elements, uranium and their secular equilibrium progenies were studied. In addition to elemental analysis, isotopic analysis was carried out for ore concentrate samples (because of being different in physical shape and their minute quantities).

MATERIALS AND METHODS

Materials

Twelve samples of unknown origin were investigated. Samples physical appearance varied between sand to fine powder form and relatively homogeneous. Two of which had typical yellow colour of ore concentrate. Three sets of samples were prepared for γ spectrometric measurements, SEM-EDX and ICP-AES and ICP-MS. For quality control purposes, IAEA reference samples were analysed parallel to the investigated samples.

For γ- spectrometric analysis

100 ml of each samples were homogenized and sealed in 200 ml plastic Marinilli and left to reach secular equilibrium between radium and its radioactive progenies. All samples were weighted and the bulk densities were determined. Absolute efficiency calibration of the system was done using mixed gamma standard reference (IAEA 368) contained in the same geometry as the samples. Samples were characterized for the following isotopes:

Isotope	Energy keV
Pb-212	221-273
Pb 214	351
Bi 214	609
Bi 214	1120
Bi 214	1765
U 235	185.7
Tl 208	583
Ac 228	338
Ac 228	911
Ac 228	968
Pa 234 m	1001

The specific parent activity used to convert activities to weights (ppm to Bq kg^{-1}) of U and Th are 12.35 and 4.06 Bq kg^{-1} respectively.

For ICP-AES measurements, Sample digestion

Sample was digested in a mixture of perchloric acid, nitric acid and hydrofluoric acid. After complete digestion, samples were heated to remove silica tetra fluoride until complete evaporation. HCl is added to dissolve the remaining part after digestion until dry, then HCl (1:1) was added and the volume of dissolved solution was diluted with distilled water. All chemicals used were of analytical grade. A series of working standards covering the range 0.5 mg/L to 10 mg /L were prepared from certified multielement stock standard solution (1000 mg /L). Working standards were analysed together with the blank and samples and calibration curve were prepared. A calibration curve is prepared every 10 samples to check for instrument accuracy. Recoveries were controlled with a known standard sample.

For ICP-MS, 200 mg of samples were dissolved using fusion with lithium tetraborate ($Li_2B_4O_7$) in platinum crucible. The final solution was made up to 100 ml diluted nitric acid where Ir as internal standard was added. The use of lithium tetraborate has proven to be a very useful way of opening out minerals associated with the rare earths, including Th and U.[5]

Methods

Initial gamma ray screening was done using gamma ray spectrometer while major elements were analysed using EDX. The used gamma ray spectrometer is Canberra inspector 2000 based on a Digital Multi channel Analyser (MCA) with a planar HPGe detector (Canberra GL0515R). The detector has a Ge crystal with 49 mm active diameter and 14.5 mm thickness, an Aluminium window of 0.5mm thickness and a measured resolution of 650 eV at 122 keV (^{57}Co) gamma energy. The output signal of the detector is processed through a Canberra preamplifier (model 2002CP).The data acquisition was carried out via gamma spectroscopy based on Canberra Genie 2000 and the isotopic composition were determined.

The ICP-AES measurements were performed using simultaneous inductively coupled plasma emission spectrometer (720 ICP-AES, Agilent Technologies). Sample were introduced via glass concentric nebulizer fitted to glass cyclonic spray chamber (single pass). An independent three-channel peristaltic pump was used for pumping the sample. High solid torch Standard (axial 2.4mm id injector) was used. The ICP-AES operating conditions were well optimized and carefully selected in order to maximize the sensitivity for the desired elements and to obtain the best precision and accuracy. Each element was measured at specific lines (nm) atomic line that gives maximum sensitivity. The intensity of this emission is indicative of the concentration of the element within the samples.

The Scanning Electron Microscope (SEM) used for investigating the swipes is Model Quanta 250 FEG (Field Emission Gun) attached with EDX Unit (Energy Dispersive X-ray Analyses), with accelerating voltage 30 K.V., magnification14x up to 1000000 and resolution for Gun.1n), FEI company, Netherlands. SEM relies on the production of a micro-focused electron beam, which is then scanned over the surface of the specimen in vacuum. When this beam of electrons strikes the sample, scattering of the beam by the surface is used to make a magnified image of the sample surface. While elastic scattering of the beam at high angles of reflection gives image in which is sensitive to high atomic weight elements (backscattered electron mode), X-ray emission by atoms in the sample gives an elemental map of the surface or the elemental composition of a single spot on the sample surface (X-ray fluorescence mode). The detection of fluorescent X-rays coming from the sample can be accomplished with a solid-state detector which measures X-rays of a wide range of energies (energy-dispersive or EDX detection). The study was focused on selected particles over several mm2

of the investigated surface using first the backscattered electron signal to locate the glowing heavy particles, then the EDX system to measure the spectrum of each particle found.

For ICP-MS analysis, a Perkin Elmer SCIEX ELAN 6000 ICP-mass spectrometer equipped with original cross-flow nebulizer was used. For uranium isotopic analysis, optimization of experimental conditions was performed for the maximum uranium ion intensity of by using a 1 µg/L natural uranium solution introduced by the nebulizer. The measured uranium isotopic ratio was corrected taking into account the mass discrimination factor.

Uranium-bearing deposits of Egypt

Egypt does not have active uranium mines. Most of the uranium occurrences in Egypt containing low-grade uranium ore, which can be extracted by Heap-leaching technique. Uranium-bearing deposits of Egypt can be classified as Pan-African younger granites (e.g., Gabal Gattar, Wadi Araba), Dyke of Felsites and Bostonites (e.g. El Atshan area), shales, Oligocene sandstones and associated rocks at Gabal Qatrani, and the carbonaceous sediments associated with Cu and Mn deposits (e.g., Wadi Araba, Abu Zeneima), phosphate deposits (e.g., Abu Tartour), black sand (in the north coast of Egypt), Sabkha deposits (e.g., in Western Desert) and siltstone of Hammamat deposits (e.g., Um Tawat in Eastern Desert). Fluorite mineralizations are widespread and associated with younger granites in the Eastern Desert of Egypt hosting uranium mineralization (Um Ara, Sella, El Aradiya, El missikat, and Gattar granite).[33]

The Egyptian Shield rocks show very wide range due to lithological variation, the younger granites show the highest radioactivity level followed by the acidic volcanic, while other rock types display the lowest radioactivity levels.[25] Fresh granite of Um Ara was reported to be of two types, according to their U and Th contents, low U (<16 ppm) low Th (<27 ppm) with Th/U ratios (1.4-2.2) and high U (16-23 ppm) high Th (42-75 ppm) with Tb/U ratios (1.8-2.4). The hydrothermally altered or mineralized granites was classified into 3 types, low U (<100 ppm) low Th (<60 ppm), moderate U (100-300 ppm) low Th (9-7 1 ppm), and high U (>300 ppm)-moderate to high (56-455 ppm). The high variations of U-contents indicate the high mobility of U during the hydrothermal stage and concentration of U under highly oxidizing conditions. The much higher mobility of U compared to Th indicates that the hydrothermal fluids were also enriched in Cl-which capable of mobilizing U only but not Th.[26] (Kepplerand Wyllie, 1990).

Extensive studies on the mineralization,[27-28] radioactive veins, whole rock trace element, rare earth in ores,[24,28] and geological and geochemical characterization of different areas in Egypt have been reported.[29] The normal granites forming Gabal Gattar are considered as an uraniferous granite type, it has U-contents ranging from 12 to 30 ppm with an average value of 18 ppm, whereas their Th-contents are within the normal value (15 ppm). Whole-rock chemical compositions of samples and radioactive vein samples with enrichment in trace elements and rare earth elements (REE) in the radioactive veins were reported by.[28]

RESULTS AND DISCUSSION

The average uranium and thorium equivalent (eU- and eTh) contents was determined for all samples. Samples S1-S10, showed eU and eTh ranging from 67- 438 ppm and 6 - 26 ppm respectively. While S11 showed ten folds higher concentration of both eU and eTh, S12 showed hundred folds of eU and as twice as eTh.

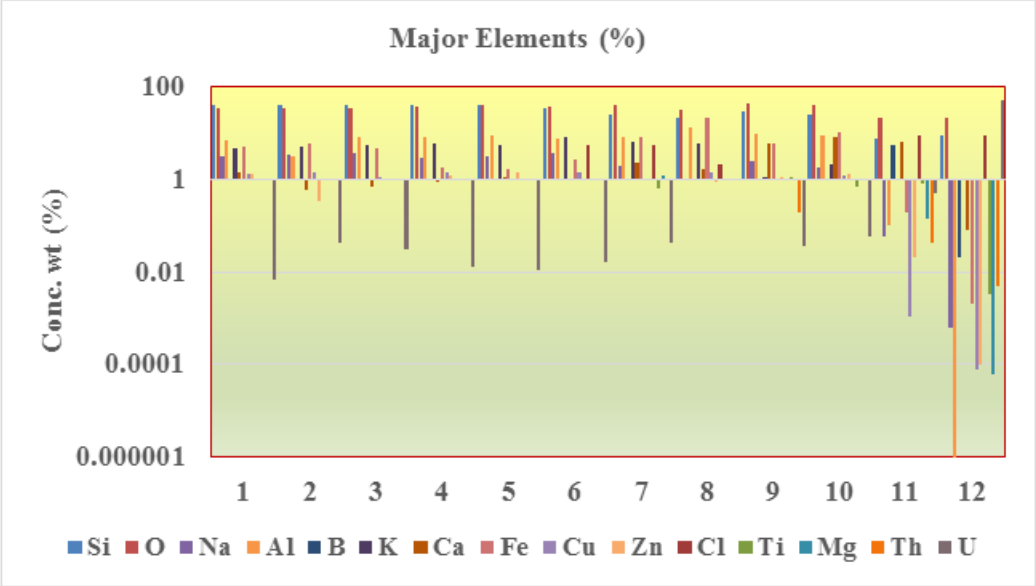

Fig 2: Concentration of major elements in (wt %) using EDX.

The concentration of major elements was determined using SEM-EDX and presented in Fig. (2). Samples, S1-S8 showed traces of Th-U (up to 0.2 wt. %) with significant contents (wt. %) of SiO_2, CaO, ZrO_2, PbO and REE (0.4). The content of Si in ten of the samples (S1-S10) ranged from about 25-40 wt. %, with an average of 33%. Na, Al, K, Ca, Fe, Zr and Cl showed averages of 3%, 8.3%, 5.1%, 2.5%, 6.8%, 0.2% and 5.8% respectively. S11 and S12 showed Zr content of 1.4 % and 29 (µg/g) respectively. Based on the physical and chemical characteristics, two-of the investigated samples could be product of process concentrates with

Si and Cl content of about 10%. Sample S12, showed the highest concentration of uranium (up to 50%) and much lower concentrations of the rest of major elements, which indicated uranium ore concentrate. In comparison to samples S1-S10, sample S11 showed relatively higher uranium content of about 0.5-wt % and lower concentrations of the rest of major elements. Fig. (3), presents the average of total trace impurities among the investigated samples. The average concentration of impurities ranged from 9 to 50%. Results suggest that samples S1 –S9 appear from the total impurities content to be of probably similar origin, S10 is of enriched vein. S11 showed higher content of trace impurities (except for Mn, Cu and Nb) in comparison to other samples and S12, which show the lowest trace and major elemental content.

Evaluations of major and minor elements indicate that S11 qualifies for a concentrate of process by-product with uranium concentration up to 0.5 wt. % and high trace impurities of about 50%, while sample S12 is an ore concentrate from different processing origin with uranium content of about 50 wt. % with 0.3 % of total impurities. This findings are consistent with literature reporting the effective and significant removal of several elements during the ADU precipitation step; these include As, Au, B, Bi, Ca, Co, Ge, Ir, K, Li, Mg, Mn, Na, Pd, Re, S, Se, Sn, Zn. Several of these elements are soluble in ammonia solution and do not form insoluble precipitates.[34]

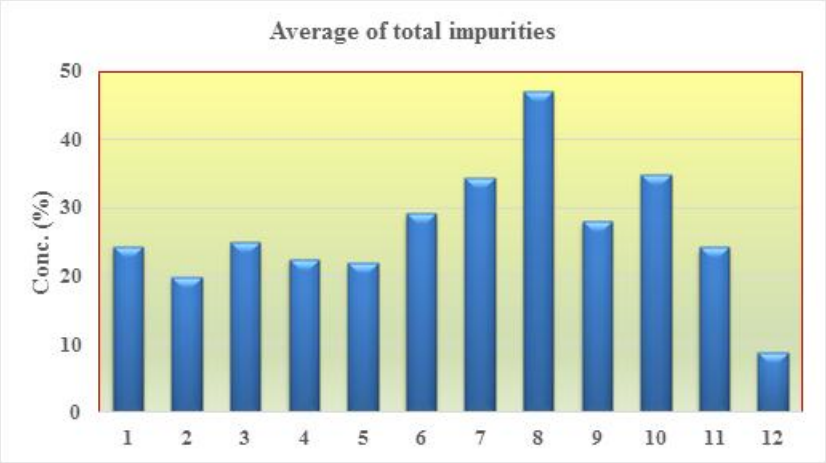

Fig 3: Average concentration (wt%) of total impurities in investigated samples.

Similar results were obtained for trace elements distribution within the twelve samples. Results suggest (propose) that samples taken from different origins and/or route-phase can show difference with regard to trace elements content. Fig. (4), shows that the distribution of trace elements in samples S1- S8 is relatively flat which indicate similar origin, where the

variation in trace elements content within one origin is expected to be lower than the variation between different origins (S10 possibly enriched vein) and/or route-phase (S11-S12).

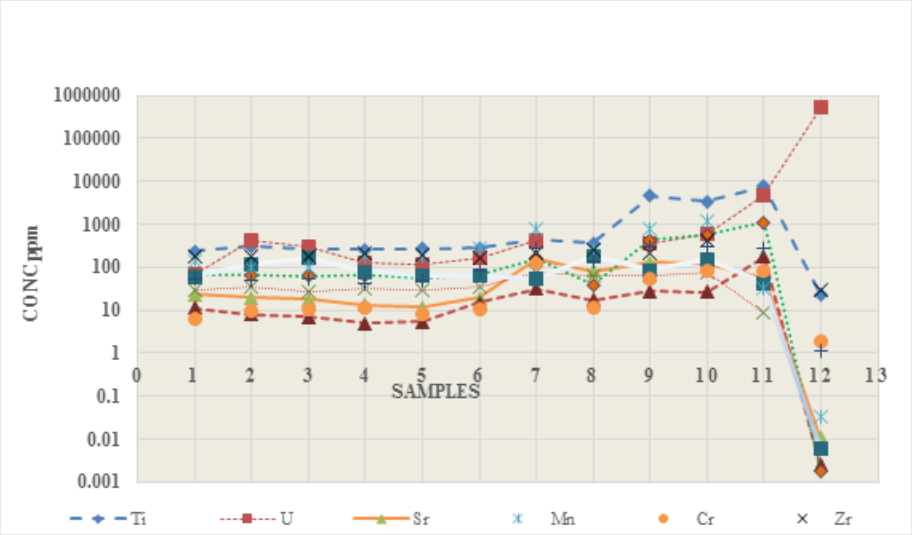

Fig 4: Signature of trace elements in investigated samples using ICP-AES.

Concentration of trace elements within samples of possible different origins varied between 50 to over 100% for U, Sr, Mn, Cr, Ni, Zn, La, Ce and 18-30% for Cu, Ti, Zr, Y and Nb, while within samples of the same origin, elements varied between 8-40% for U, Sr, Mn, Cr, Ni, Zn, La, Ce and 4.5-25% for Cu, Ti, Zr, Y and Nb.

To eliminate the variation in concentrations of elements, concentrations were normalized to the average concentration among investigated samples. This shows the range of variation for each element within investigated samples in relation to their origin. Fig. (5), presents the variation in trace elements concentrations normalized to the average in samples measured by ICP-AES.

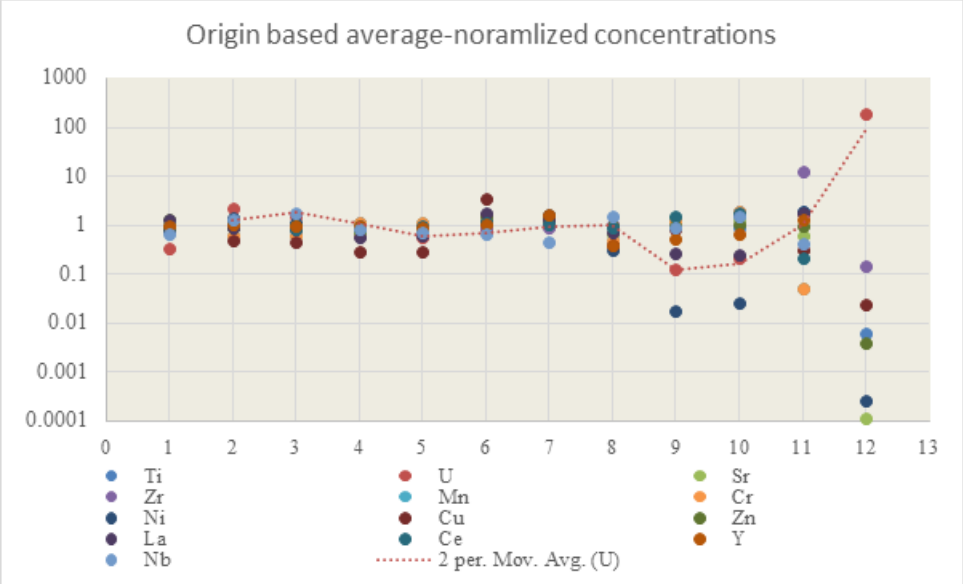

Fig 5: Trace elements values average-normalized concentrations.

The average-normalized values varied between 1±1 except for U concentrate in S12, Zr enrichment in S11 and Cu anomaly in S6. Values for samples S1-S8 showed narrower variation in comparison to samples S11-S12. In comparison to samples S1-S10, sample S11 showed elevated concentrations in Y, Ce, La, Ni, Cr, Zr, Ti and U confirming our previous findings. Concentrations of several elements may increase significantly during processing and portioning steps where uranium is simply a by-product to waste stream. This explains the elevated concentrations of trace elements in S 11. Some of which might also be due to contamination during processing. Generally, concentration of major elements determined by EDX were within 20% in agreement with ICP-AES and ICP-MS.

Literature reported the use of REE abundance patterns as predictive signatures. To eliminate variation in concentrations of elements, concentrations were normalized to a reference concentration such as the average chondritic meteorites. This shows the pattern of each element or group of elements in connection to their origin.[13] Fingerprinting of the REE contents of the investigated sample is presented in Fig 6 as normalized REE concentrations to the reference chondrite.

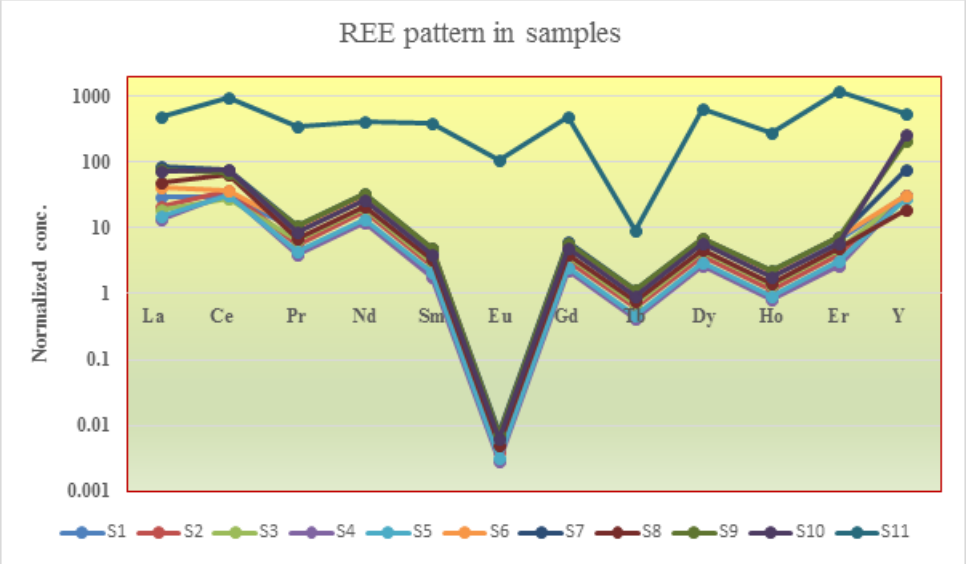

Fig 6: Chondrites normalized REE distribution print in investigated samples.

The pattern of REE within investigated samples was almost identical proposing common geological origin of samples. Samples (S1-S10) showed slight enriched pattern in *light REE* (LREE) La, Ce, Pr, Nd, with strong *negative Eu* and depletion in Ho and Tb. Results have shown that the origin of samples could be derived from deposits of the same genetic type. The REE pattern resembles quartz-pebble conglomerate UOC samples reported in literature. The *negative Eu* anomaly seen for analysed samples can be attributed to the presence of Eu^{2+} in a reducing magma. This enables Eu^{2+} to substitute Ca^{2+} and indicate fractionation in igneous systems crystallizing controlled by melt crystal chemistry and redox potential.[19] This suggests a granitic primary source of REEs that occurs in trivalent oxidation state (except for Ce^{4+} and Eu^{2+}) with decreasing ionic radii from La to Lu and minor differences in their fractionation pattern (Li et al. 2013).[32] Sample S11, showed higher content in all REE within two order of magnitudes, flat LREE pattern and enriched heavy REE which propose that the origin could be phosphorite ore. Based on the concentration of other trace elements and uranium content (up to 0.5%), the sample is most likely by-product of phosphate processing. Results confirm that REE and some trace elements abundances provides information about the geological formation conditions of the source ore and are not significantly altered by ore processing.

The relation between U-REE in ore samples and respective concentrates are presented in Fig. (7).

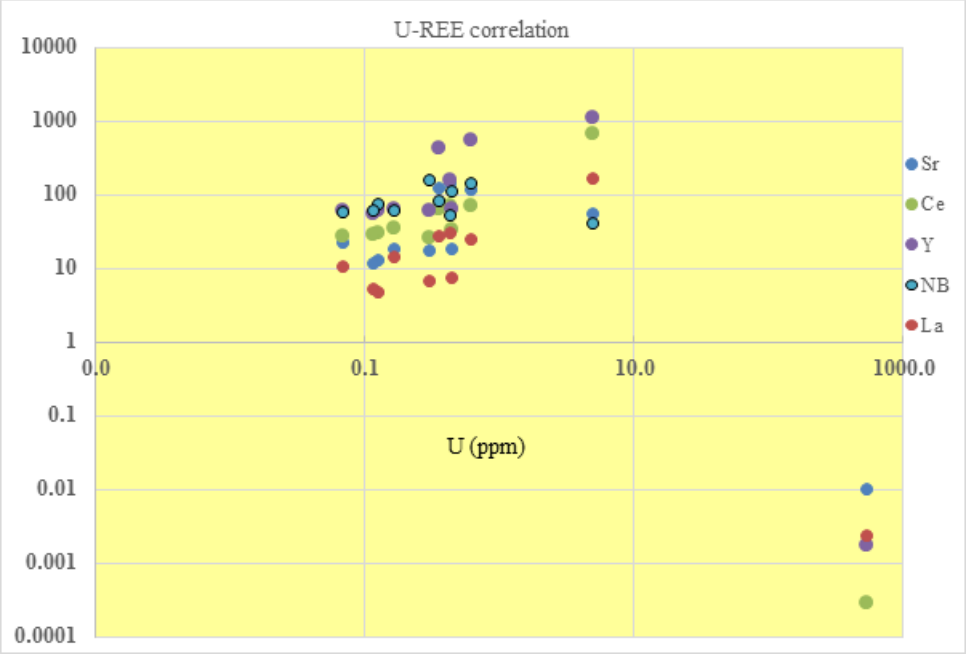

Fig. 7: U-REE correlation of ore samples and respective ore concentrate.

The correlation shows distinctively three sets of variation, S1-S10, S11 and S12 which confirms the common origin of samples S1-10 with minor inter-changes, S11 with elevated concentration as ore processed by-product and S12 with high U content and low content of REE. Results propose that elemental content of Sr, Nb, Y and Ce can also provide complementary geolocation information.

As S11 and S12 are products of concentration and separation processes with high uranium content, isotopes of uranium, thorium and some stable isotopes were investigated further. Both samples showed natural uranium with ^{235}U content of 0.727±0.05. The dates of production of S11 and S12 were determined using the $^{230}Th/^{234}U$ dating method. Results propose that production dates are 19 and 30 years respectively. Fig. (8), shows the isotopic ratio of $^{230}Th/^{234}U$, $^{235}U/^{231}Pa$ and $^{228}Th/^{232}Th$.

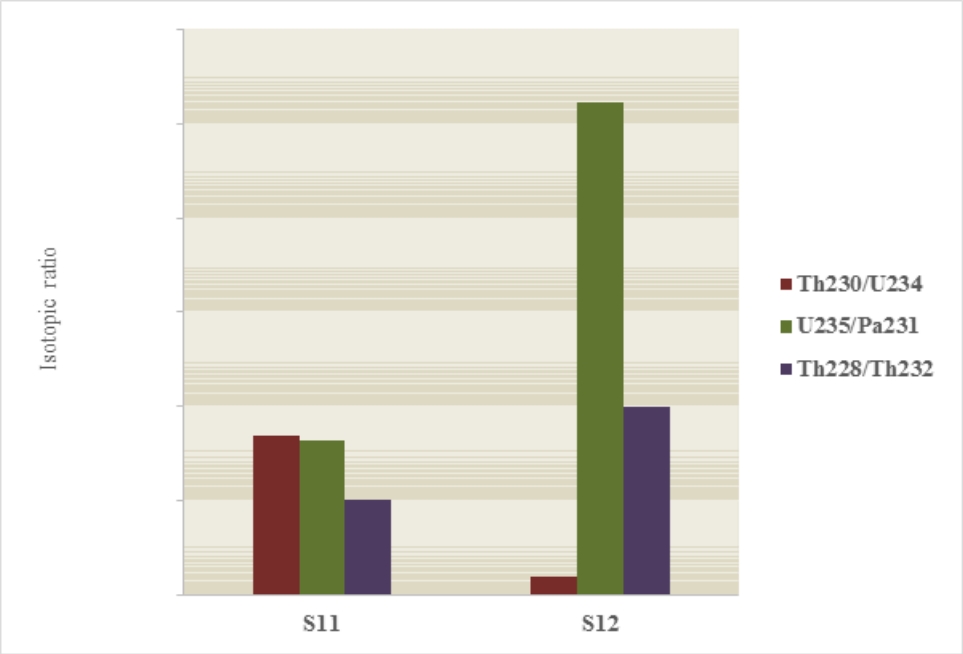

Fig. 8: Isotopic ratios of $^{230}Th/^{234}U$, $^{235}U/^{231}Pa$ and $^{228}Th/^{232}Th$.

Considering the impurity content and pattern especially of several alkali earth elements in the final product, we believe that S12 is a product resulting from carbonate-based heap leaching process. Sulphuric acid leaching would have had higher separation factor through the formation of insoluble Sulphate precipitate. This might have been a disadvantage for the age determination based on the $^{228}Th/^{232}Th$ chronometer, where the complete radium separation from thorium is the major condition for use. The difference in isotopic ratios of some stable isotopes is presented in Fig. (9).

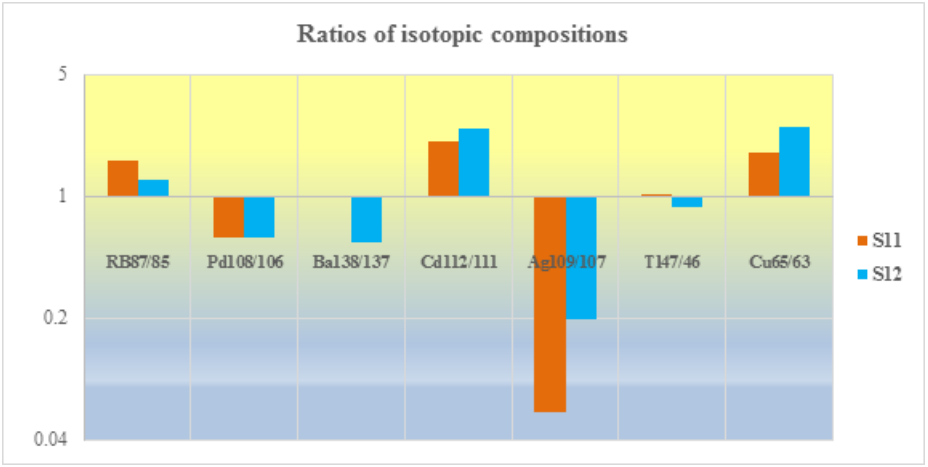

Fig. 9: Isotopic ratios of selected stable isotopes in concentrate products.

Ratio of S12/S11 for Ti, Mo, Zr and Nb were in the order of 10^{-4} showing significant separation during purification steps. Differences between S11 and S12 could be due to the fractionation occurring during leaching of the ore minerals and their different chemical and isotopic composition.

CONCLUSION

In the absence of extensive database, providing information on classification of potential uranium ores, uranium concentrate and other ore concentrates, investigation of unknown samples is a very complex task. The ambiguity of geological origin of investigated samples and the process used to produce ore concentrate were technically very challenging. Based on the physical appearance and the preliminary screening using Gamma Spectrometry measurements, it was possible to distinguish ten rock samples and one uranium ore concentrate. Nevertheless, uranium-bearing deposits in Egypt can be many, which has also complicated the possibility to identify the origin based on single technique. The content of major elements and the average of total trace impurities between the investigated samples were a mean to focus the searching especially towards the genetic origin of the geological samples. The use of normalized REE concentrations to the reference chondrite revealed almost identical pattern proposing common geological origin of samples. Hereafter, it was extremely supportive to predict the possible geological origin. The study suggests that, this pattern resembles quartz-pebble conglomerate. It is also believed that the ore concentrate is resulting from carbonate-based heap leaching process. The use of isotopic ratios of Sr, Pb, etc, in the processed material was not always possible. Due to the high content of uranium and other abundant elements, sample was significantly diluted which affected the detection limit of some minor elements. The future is to compile all the analysis information of each stage and patterns in a national database including the possible uranium ore concentrate production processes to illustrate the behavior of the signatures and validate the effectiveness in nuclear safeguards and forensics.

REFERENCES

1. IAEA, INFCIRC 153, corrected.
2. ASTM International Standards, C967-08, (2008), Standard specification for Uranium Ore Concentrate, DOI: 10.1520/C0967-08.

3. Varga, Z., Wallenius M. and Mayer, K., (2010), Origin assessment of uranium ore concentrates based on their rare-earth elemental impurity pattern, Radiochemica Acta, 98(12).
4. Brennecka, G. a., Borg, L.E., Hutcheon, I.D., Sharp, M. a., Anbar, A.D., (2010), Natural variations in uranium isotope ratios of uranium ore concentrates: understanding the 238U/235U fractionation mechanism. Earth Planet Sci. Lett., 291: 228–233. http:// dx.doi.org/10.1016/j.epsl.2010.01.023.
5. Han, S.-H., Varga, Z., Krajkó, J., Wallenius, M., Song, K., Mayer, K., (2013), Measurement of the sulphur isotope ratio (34S/32S) in uranium ore concentrates (yellow cakes) for origin assessment. J. Anal. At. Spectrom, 28: 1919. http://dx.doi.org/10.1039/ c3ja50231g.
6. Krajkó, J., Varga, Z., Yalcintas, E., Wallenius, M., Mayer, K., (2014), Application of neo-dymium isotope ratio measurements for the origin assessment of uranium ore con-centrates. Talanta, 129: 499–504.http://dx.doi.org/10.1016/j.talanta.2014.06.022.
7. Keegan, E., Richter, S., Kelly, I., Wong, H., Gadd, P., Kuehn, H., Alonso-Munoz, A., (2008), The provenance of Australian uranium ore concentrates by elemental and isotopic analysis. Appl. Geochem, 23: 765–777. http://dx.doi.org/10.1016/j.apgeochem. 2007.12.004.
8. Keegan, E., Wallenius, M., Mayer, K., Varga, Z., Rasmussen, G., (2012), Attribution of uranium ore concentrates using elemental and anionic data. Appl. Geochem, 27: 1600–1609. http://dx.doi.org/10.1016/j.apgeochem.
9. Mayer, K., Wallenius, M., Ray, I., (2005), Nuclear forensics–a methodology providing clues on the origin of illicitly trafficked nuclear materials. Analyst, 130: 433–441. http://dx. doi.org/10.1039/b412922a.
10. Svedkauskaite-LeGore, J., Mayer, K., Millet, S., Nicholl, A., Rasmussen, G., Baltrunas, D., (2007), Investigation of the isotopic composition of lead and of trace elements concentrations in natural uranium materials as a signature in nuclear forensics. Radiochim. Acta, 95: 601–605.
11. Svedkauskaite-LeGore, J., Rasmussen, G., Abousahl, S., Van Belle, P., (2008), Investigation of the sample characteristics needed for the determination of the origin of uranium-bearing materials. J. Radioanal. Nucl. Chem., 278: 201–209.
12. A.C. Keatleya,∗, P.G. Martina, K.R. Hallama, O.D. Paytona, R. Awberyb, F. Carvalhoc, J.M. Oliveirac, L. Silvac, M. Maltac, T.B. Scotta, Source identification of uranium-containing materials at mine legacy sites in Portugal. Available (2018), Journal of

Environmental Radioactivity 183: 102-111, https://www.researchgate.net/publication/322504961_Source_identification_of_uranium-containing_materials_at_mine_legacy_sites_in_Portugal.

13. Taylor S. R. and McClennan S. M. (1985), The Continental Crust: Its Composition and Evolution, Blackwell, Oxford, 312.
14. Kenton, JMoody, Patrik M. Grant and Ian D. Hutcheon, (2015), Nuclear Forensic Analysis, isbn: 978-1-4398-8061-6, crcpress.com.
15. Knaack, C., Cornelius, S.B. and Hooper, P.R., (1994), Geo-Analytical Lab, Washington State University.
16. Uranium resources and reserves in Egypt, (2017), DOI: 0.13140/RG.2.2.17312.69124, Conference: Department of Geology; Faculty of Sciences; Tanta University.
17. Abdel Maguid, A.A., (1986): Geologic and radioactive studies of uraniferous granites in Um Ära- Um Shilman Area, Southeastern Desert, Egypt. Ph.D. Thesis, Suez Canal University.
18. Ibrahim M. E. (2002), Occurrence of uranium in bearing minerals in Um safi pyroclastics, central Eastern Desert, egyptian Jornal og geology, 46(1).
19. Kamaleldin M. Hassan, Trace elements and REE enrichment at Seboah Hill, SW Egypt, (2018), MINERALOGIA, 49(1-4): 47-65. DOI: 10.2478/mipo-2018-0007. https://www.researchgate.net/publication/327677429_Trace_elements_and_REE_enrichment_at_Seboah_Hill_SW_Egypt
20. S. Shawky, H. Amer and M.I. Hussin, (2000), Information on low level Radiation – a samples of data and calibration difficulties- a case study performed by NCNSRC in Egypt, Proceeding of the 5th International Conference on high levels of natural radiation and radon areas, radiation dose and health effects, Munich, Germany.
21. M.Ryzhinskiy, (2008), Evaluation of the trace element analysis results of UF6 samples from Libya. Report IDS1-365/08, 1-8.
22. Fleischer, R.L., Raabe, O.G., (1978), Recoiling alpha-emitting nuclei. Mechanisms for uranium-series disequilibrium. Geochim. Cosmochim. Acta, 42: 973–978.
23. Ovaskainen, R., Mayer, K., De Bolle, W., Donohue, D., De Bievre, P., (1997), Unusual Isotope abundances in natural uranium samples. In: Foggi, C., Genoni, F. (Eds.), Proceedings of the 19th Annual Symposium Safeguards and Nuclear material Management, Montpellier, Ispra, ESARDA No. 28.

24. Leanne M. Mallory-Greenough and John D. Greenough, (2004), Whole-rock trace-element analyses applied to the regional sourcing of ancient basalt vessels from Egypt and Jordan, Can. J. Earth Sci., 41: 699–709.
25. H. Z. Harraz, Uranium Ore Deposits., (2013), https://www.researchgate.net/publication/301865112_Uranium_Ore_Deposits.
26. H. Keppler and P. J. Wyllie, (1990), Role of fluids in transport and fractionation of uranium and thorium in magmatic processes, Nature, 348(6301).
27. Ibrahim, M. E, Aly, G. M. and El-Tohamy, A.M., (2012), Mineralogical and Geochemical Aspects of Nubia Sandstons at Gabel El Ghurfa, Southeastern Desert, Egypt, Arab Journal of Nuclear Sciences and Applications, 45(2): 117-129.
28. M. E. Ibrahim, G. M. Saleh and W. S. Ibrahim, (2010), Low grade metamorphosed sandstone-type uranium deposit, Wadi Sikait, South Eastern Desert, Egypt, Journal of Geology and Mining Research, 2(6): 129-141.
29. Hesham M Kamal, (2017), Rare Earth Elements Resources and Different Recovery Techniques from Egyptian Ores, Biomed J Sci & Tech Res, ISSN: 2574-1241, DOI: 10.26717/BJSTR.2017.01.000550.
30. Maher I. Dawoud, Gehad M. Saleh, Hassan A. Shahin, Farrage M. Khaleal and Bahaa M. Emad, (2018), Younger Granites and Associated Pegmatites of Gabal El Fereyid – Wadi Rahaba Area, South Eastern Desert, Egypt: Geological and Geochemical Characteristics, Geosciences Research, 3(4).
31. Varga, Z., Wallenius, M, Mayer, K. and Meppen, M., (2011), Analysis of uranium ore concentrates for origin assessment, J. Radiochimica Acta, 1: 1-4.
32. Li CS, Shi XF, Kao SJ, Liu YG, Lyu HH, Zou JJ, Liu SF, Qiao SQ, (2013), Rare earth elements in fine-grained sediments of major rivers from the high-standing island of Taiwan. J Asian Earth Sci, 69: 39–47.
33. Nasser, M., Mahmoud Shalaby and Hassan M. Helmy, (2013), Trace and REE element geochemistry of fluorite and its relation to uranium mineralizations, Gabal Gattar Area, Northern Eastern Desert, Egypt Arabian Journal of Geosciences, DOI: 10.1007/s12517-013-0933-2.
34. Varga, Z., Judit Krajkó, Maxim Peńkin, Márton Novák, Zsuzsanna Eke, Maria Wallenius, and Klaus Mayer, (2017), Identification of uranium signatures relevant for nuclear safeguards and forensics, J Radioanal Nucl Chem, 312(3): 639–654. Published online 2017 Apr 20. doi: 10.1007/s10967-017-5247-5 PMCID: PMC5446562, PMID: 28596631